G.F. Carnevale[+] and R.C. Kloosterziel[o]

Stability of Isolated Compound Vortices

Abstract

The stability of the members of a class of isolated vortices is discussed. Two well-known examples of stable isolated flows are the dipole and tripole. The existence of an even more complicated stable isolated flow is demonstrated here. Like the dipole and tripole, it is also a compound vortex and consists of a core vortex surrounded by three satellite vortices of opposite sign. The core of this 'quadrupole' is triangular in shape and the satellites are semicircular. The stability of this flow is inferred from high-resolution numerical simulations and analysis of point-vortex models. Further consideration suggests that all higher order n-poles will be unstable to merger of the satellite vortices.

Introduction

Isolated two-dimensional vortices are models for the localized flow structures that are prevalent in geophysical flows. By isolated we mean a vortex whose net circulation is zero so that the velocity field induced by the vortex falls off faster than $1/r$ in the far field, where r is the distance measured from the center of the vortex. Such vortices are created, for example, by topographic forcing of islands or mountains, instabilities of major current systems such as the Gulf Stream, and strong localized wind forcing on the ocean surface. Two-dimensional models provide a first approximation to such vortices and have been extensively studied.

A simple model for circularly symmetric isolated flows consists of a core of single-signed vorticity surrounded by an annulus of vorticity of opposite sign, with amplitudes such that the total circulation vanishes. There have been numerous studies of the stability and evolution of such vortices. If the annulus is sufficiently narrow, so that the fall off of vorticity from its maximum to minimum value is sufficiently steep, then the flow is unstable. Numerical simulations and laboratory experiments (cf., Carton & McWilliams 1989, Kloosterziel & van Heijst 1991, Carnevale & Kloosterziel 1994) show that under these conditions the vorticity regions can break up and reassemble into more complex, yet more stable, structures. One common scenario is the formation of a tripole. In that case the core becomes elliptical in shape while the annulus clumps and separates into two distinct vortices that remain as satellites of the core. The entire compound vortex simply rotates, as in solid-body rotation, at a constant angular rate about the centre of the core. Another common scenario, called dipole splitting, results if the initial profile is even steeper than for the case which produces the tripole. The instability then proceeds initially as in the case of tripole formation, but eventually the satellites shear apart the core, which then rolls up into two new vortices. This results in two dipoles that propagate away from each other.

The dipole consists of two oppositely-signed vortices that advect each other, and it appears to be a very stable structure. The well-known analytic model for this flow was given by Lamb (1932), and many writers, therefore, refer to it as the Lamb dipole. Recently, reference to an earlier publication (Chaplygin, 1903) of this analytic model has been made, but we have not yet seen a copy of this work.† This dipole model has been of considerable interest since it can be used to represent various geophysical phenomena such as mushroom vortices (cf., Federov 1989). Furthermore, this dipole has a generalization to a similar isolated flow on the β-plane, called the modon, and as such has generated considerable interest due to its possible relevance in the phenomenon of atmospheric blocking (cf., Stern 1975, McWilliams 1980). In numerical simulations and laboratory experiments, the dipole appears to be very stable. Diagrams summarizing the stability of the modon to various types of perturbations have been published by McWilliams *et al.* (1981) and Carnevale *et al.* (1988a). It is hard to give a precise stability range because much depends on the exact form of the perturbation, but it seems that modons are most sensitive to forcing on length-scales comparable to their own diameter and that perturbations of greater than 10%, relative to its unperturbed strength, are necessary for destruction. The usual instability by which the modon is destroyed involves a separation of the two regions of oppositely-signed vorticity (Carnevale *et al.* 1988b). Similar studies of the Lamb dipole show essentially the same results as in the modon case (unpublished). Although there have been many attempts at proving the stability of dipoles, an uncontested proof remains elusive (cf., Carnevale *et al.* 1988c, Nycander 1992).

An even more complicated isolated flow is the tripole. It consists of a central core of vorticity of one sign and two satellites of opposite sign, all co-linear and all rotating at constant rate about the center. Although this compound vortex appeared in a published numerical simulation of turbulence (Sadourny, 1985), it was not noted in that paper or any other, to our knowledge, until the work of Legras *et al.* (1988), in which the tripole was clearly pointed out as being a very stable element in an otherwise turbulent flow. Publications of laboratory work which also showed this tripole quickly followed (van Heijst & Kloosterziel, 1989). In that work, the tripole was produced as a result of the breakdown of a circularly symmetric flow as discussed above. Oceanic observations of a tripole were reported by Pingree & LeCann (1992). Laboratory studies (van Heijst *et al.* 1991) and numerical simulations (Polvani & Carton 1990) attest to the

† Note added in proof: Chaplygin's work is described in a recent paper by Meleshko & van Heijst (1994), *J. Fluid Mech.* **272**, 157–182.

stability of these structures. Unfortunately, there is no analytic model of tripoles with continuous vorticity. Models using three point vortices have been successful at simulating many of the properties of the tripole under external perturbations, and nonlinear stability of this three point model with respect to displacements of the satellites can be proven (Kloosterziel, 1990).

At this point, it is natural to consider whether there may be a hierarchy of more complicated stable n-poles consisting of a core vortex surrounded by $n_s = n - 1$ satellites of opposite sign. In fact, laboratory experiments on the instabilities of circularly symmetric vortices in a rotating tank (Kloosterziel & van Heijst 1991) have shown the natural evolution of a quadrupole consisting of a triangular core vortex surrounded by three semi-circular satellites of vorticity of opposite sign. Although never observed in other than a transitory state in the laboratory, subsequent numerical simulations and point vortex models led us to believe that this kind of structure can also be stable if prepared in a sufficiently symmetric way. This is further discussed in the next section.

As for the existence of compound vortices even more complicated than the quadrupole, our investigations indicate that there are none. The instability of the higher-order structures is discussed in a separate section below.

The quadrupole or triangle vortex

In rotating-tank experiments, the quadrupole is observed to break apart rather rapidly after it has formed (see Kloosterziel & van Heijst 1991, Carnevale & Kloosterziel 1994). The instability begins with two of the satellites moving closer together. One of these satellites moves in between the other satellite and the core. The two satellites are then close enough together to merge into a single vortex in the same way that two like-signed vortices merge in isolation (cf. Melander *et al.* 1988). This results in a transitory tripole stage, which then proceeds to double-dipole splitting as described above. Orlandi & Van Heijst (1992) were able to capture this formation and transitory existence of the quadrupole in numerical simulations. This encouraged us to explore more fully the mechanisms involved in this evolution, using spectral simulations and point-vortex models.

Orlandi & van Heijst (1992) used the following vorticity profile as their unperturbed basic state:

$$\zeta = -\left(1 - \frac{1}{2}\alpha r^{\alpha}\right)\exp(-r^{\alpha}), \tag{1}$$

where r is the radial distance from the centre of the vortex. Distances have been non-dimensionalized by L, the horizontal length-scale of the vortex, and velocities by U. This is the same profile as used in several earlier studies (e.g., Carton & McWilliams, 1989). Note that increasing α makes the vorticity in the core more uniform, the width of the annulus smaller, and the slope of the vor-

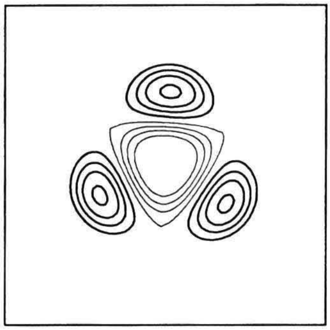

Fig. 1. Vorticity contour plot of a quadrupole vortex. Thick (thin) contours indicate positive (negative) relative vorticity. The contour level values are chosen to have increments of $\Delta\zeta = 0.2\ \mathrm{s}^{-1}$. The dimensional velocity and length scales used in the initialization were $U = 20$ cm/s and $L = 11$ cm, and the length of a side of the computational domain was 90 cm (although here we have only plotted the field over an inner square of 54 cm on a side).

ticity as a function of r steeper between the core and annulus. We will refer to α as the steepness parameter. This family of profiles is a reasonable model for the types of isolated vortices created in the tank. Orlandi & van Heijst (1992) used an initial condition in which the basic state in equation (1), with $\alpha = 5$, is perturbed with a randomly generated vorticity field defined by

$$\zeta' = \eta \exp\left(\frac{-(\alpha r^{\alpha} - 2)^2}{2\sigma^2}\right) - c. \tag{2}$$

Here $\eta(x, y)$ is a random number uniformly generated on the range $(-\eta_0, \eta_0)$ for each grid-point, and c isa constant chosen to ensure that the spatially integrated value of ζ' (i.e. the circulation of the perturbation) vanishes. This perturbation is concentrated at the radius where the unperturbed vorticity field changes sign, and σ can be adjusted to make the perturbation penetrate the core and annulus to any desired degree.

In Carnevale & Kloosterziel (1994), we examined the stability of the vorticity distribution (1) for a range of α-values, subject to perturbations of single azimuthal modes given by

$$\zeta' = \mu \cos(m\theta) \exp\left(\frac{-(\alpha r^{\alpha} - 2)^2}{2\sigma^2}\right), \tag{3}$$

where μ is a constant amplitude and m is the mode number. The results of a linear stability analysis showed that the behaviour observed in the laboratory experiments and the random initial condition simulations could be understood as a combination of the simultaneous growth of both azimuthal modes $m = 2$ and $m = 3$. Furthermore, setting $\alpha = 6$, we found that if modes other than mode 3 are sufficiently weak initially, a symmetric quadrupole can form and persist.

In a simulation with an initially pure mode-3 perturbation and with viscosity appropriate to the rotating-tank conditions used in the laboratory experiments, we found that a fairly symmetric triangular core forms by the end of the first rotation. It also takes about one rotation for the triangle to form in the purely inviscid case but the rotation period is about 15% shorter. Figure 1 shows the triangle structure in the viscous simulation after about two full rotations. The fact that it is not perfectly three-fold symmetric is due to asymmetries associated with the finite resolution of the grid which have amplified during the evolution. This quadrupole persisted unchanged in form although becoming somewhat broader in scale due to the effect of the Laplacian diffusion. During the course of the simulation the amplitude of the vorticity field decayed by three orders of magnitude under the influence of Ekman drag and molecular diffusion. This indicates that it should be possible to create a triangle vortex in the laboratory which would simply decay in amplitude.

To test the inviscid stability of the quadrupole, we began with the quadrupole shown in figure 1 as an initial condition and simulated forward in time with no viscosity. In figure 2, we show the initial stream function in the reference frame co-rotating with the quadrupole. If the state were perfectly stationary, then these streamlines would be aligned with those of the vorticity. Since there is some difference, this quadrupole deviates from an ideally symmetric one that would be steadily rotating; nevertheless, we followed the inviscid evolution of this vortex for over twenty of its rotations without observing any evidence that it would break down. This was verified at both resolutions 64×64 and 128×128. Although there was some variation of its form over that long period, the basic structure did not change significantly. Thus it appears possible that, for inviscid flow, the symmetric quadrupole is a stable structure. The difficulty in finding a stable triangle vortex experimentally or in the corresponding random-perturbation simulations must be due to the fact that it is only stable for perturbations with amplitude below some small threshold value.

To examine how large the tolerance for perturbations is, we performed two different kinds of stability tests. In the first, we perturbed the strength of the

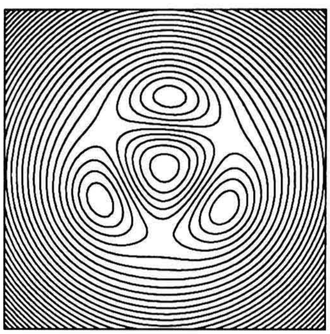

Fig. 2. Stream function contour plot of quadrupole vortex. The stream function is evaluated in the co-rotating frame with rotation period 81s. The contour increment was taken as $\Delta\Psi = k^2\,\Delta\zeta$, where $k = j_1^1/a$ with $j_1^1 = 3.83$ and where $a = 12$ cm is approximately the radius of the semicircular satellites.

satellite vortices while leaving the inner triangular core unperturbed. This type of perturbation was suggested by an analysis of point-vortex models and by experience from the experiments and simulations. It seemed that the triangle is sensitive to variations in the strengths of the outer satellites. Such asymmetries would lead to variations in the rate of revolution of the satellites about the core and thus permit a collision of a pair of satellites. The perturbation was prepared by taking the state shown in figure 1 and multiplying the vorticity field of the satellites by the factors $1+\delta$, $1-\delta$, 1, respectively, in one set of experiments, and by factors $1+\delta$, $1-\delta/2$, $1-\delta/2$, in a second series. All of the stability simulations were run with no bottom drag and no Laplacian viscosity; however, in order to avoid the build up of enstrophy in the smallest scales during the long runs, hyperviscosity was used.

In figure 3, we plot the time it takes until a merger occurs between two of the satellites in each of these series of experiments. The time is given in units of the rotation period of the unperturbed vortex and the simulations were terminated after 20 rotation periods even if no breakdown had occurred. For perturbations less than 2 percent, the triangle remains intact for more than 20 rotation periods. There is a steep fall off of the time to merger or breakdown between perturbations of 2 and 4 percent. Defining a stability boundary based on simulations requires some arbitrary choice of how to define the stable regime since numerical noise will eventually contaminate the results. For practical purposes, we can take our stability boundary to be approximately where the lifetime, as a function of the perturbation amplitude, becomes very large. Thus the stability boundary is around 3 percent. This is much smaller than the rough estimate of about 10% for dipoles as mentioned above.

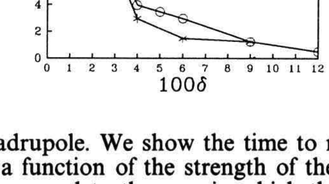

Fig. 3. Stability plot for the quadrupole. We show the time to merger of two of the satellites for the perturbed triangle vortex as a function of the strength of the perturbation. The data points marked by asterisks (circles) correspond to the case in which the initial satellite vortex strengths are multiplied by $1+\delta$, $1-\delta$, 1 ($1+\delta$, $1-\delta/2$, $1-\delta/2$). The merger time is expressed in units of the unperturbed vortex rotation period (81 s).

In the second kind of stability study, we added a randomly generated homogeneous isotropic vorticity field to the vortex shown in figure 1. This perturbation field was created by adding contributions from all wavevectors with wavenumbers between two fixed limits, $k_0 \leqslant k_1$, in such a way that the energy spectrum of the perturbation was independent of wavenumber in that band. The real and imaginary parts of the complex amplitude for each wave number were generated from a Gaussian distribution. The perturbation amplitude is measured as the ratio of the rms velocity of the perturbation to the rms velocity of the triangular vortex. The rms averages are taken only over the area within an imaginary boundary of an idealized structure consisting of the triangle surrounded by three semicircles. The length scale of the perturbation is defined as $\lambda \equiv L_B/(L_\Delta \bar{k})$, where L_B is the size of the periodic computational box, $L_\Delta = 2a$ is the length of one side of the triangle vortex, and $\bar{k} = (k_1 + k_0)/2$. Thus the value $\lambda = 1$ corresponds approximately to the scale of the triangular vortex. The circles on the plot in figure 4 indicate the simulations in which the triangle vortex survives for more than ten rotation periods, and the asterisks indicate the simulations in which the triangle breaks up before that time limit is reached. Again the definition of a stability boundary is somewhat fuzzy. But we may conclude that the triangle vortex is most unstable to perturbations of length scale close to its own, and the minimum strength of the perturbation needed to destabilize it is about 3 percent measured in rms velocity. The structure appears very stable to large-scale perturbations, which for the most part simply advect it, and also to small-scale perturbations, which are quickly sheared out to even smaller scales to be eventually dissipated by hyperviscosity.

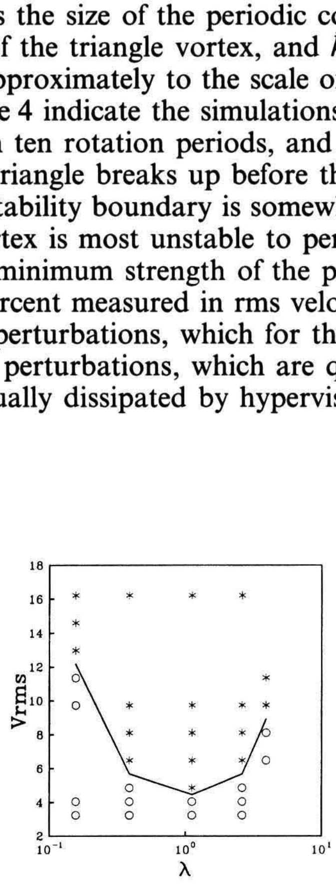

Fig. 4. Stability plot for the quadrupole. The graph shows the results from a stability study in which a random velocity field of length scale λ and amplitude V_{rms} was added to the triangle vortex. Asterisks mark the experiments in which merger occurred between two of the three satellites before ten rotations periods of the unperturbed structure had elapsed. Circles mark those simulations in which the vortex system was still intact after ten rotation periods. The perturbation amplitude V_{rms} is given in multiples of the rms velocity of the triangle vortex, and λ is defined so that $\lambda = 1$ corresponds to the size of one side of the triangle vortex (see text).

Higher order n-poles

Since the mode 3 instability of the initially circularly symmetric vortex leads through nonlinear saturation to the triangular vortex, we went on to test whether the mode 4 instability would lead to a square vortex. We performed a series of experiments with values of α running from 3 to 8, both with and without viscosity. To the unperturbed state we added a perturbation as defined by equation (3) with azimuthal wavenumber 4 only, with amplitudes varying from $\mu = 0.1$ to 0.5 and with a length-scale $\sigma = 1$ in the initial condition. A further exploration of the parameter space was not performed since we found that these somewhat arbitrary choices did lead to the formation of square vortices for $\alpha > 5$. For example, in figures 5 and 6, we show the vorticity and stream function plots of a square vortex which formed for a steepness parameter $\alpha = 8$. The simulation which produced this vortex was run with Ekman decay time and molecular viscosity set to the values that agreed with our laboratory experiment that produced quadrupoles (i.e., $T_E = 132$ s and $\nu = .01$ cm^2/s). The basic structure developed by time $t = 10$ s and by time 72 s, the structure reached the state shown in the figure. The vorticity distribution is shown in figure 5 and the stream function, in the co-rotating frame of the vortex system, is given in figure 6.

In all the simulations in which the square vortex formed, the structure broke down before at most 3.5 rotations were completed. The longest-lived square vortex was achieved for $\alpha = 8$, starting with a perturbation amplitude of $\mu = 0.5$, with only hyperviscosity dissipation acting. In all cases, these square vortices, which have satellites of equal strength, broke down through the simultaneous merger of their satellites in two pairs on opposite sides of the square core.

In figure 7, we show the instability that destroys the square vortex. The conditions for the simulation were again set to match those in our rotating tank experiments. The initial vortex in this simulation was created with $\alpha = 8$, and a

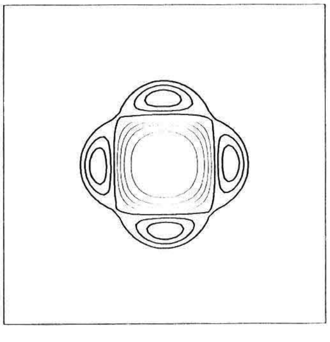

Fig. 5. Vorticity contour plot of a square vortex. Thick (thin) contours indicate positive (negative) relative vorticity. The contour level values are chosen to have increments of $\Delta\zeta = 0.3$ s^{-1} (other parameters are as in figure 1).

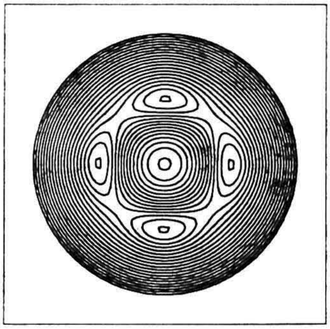

Fig. 6. Stream function contour plots of a square vortex. The stream function is evaluated in the co-rotating frame with rotation period 44.8 s. Beyond a certain value, the high level contours were not drawn because of 'bleeding' between the lines. The contour increment was taken as $\Delta\Psi = k^2 \Delta\zeta$, where $ka = j_1^1$ and $a = 8.3$ cm is approximately the radius of the semicircular satellites (other parameters are as in figure 1).

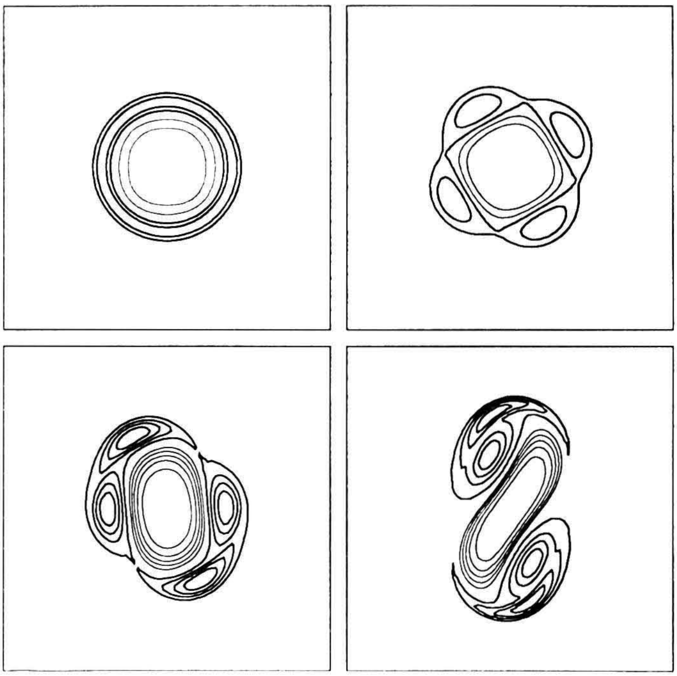

Fig. 7. Vorticity contour plot showing the evolution of the square vortex. For this simulation we used a kinematic viscosity and bottom drag with an Ekman decay time typical of the values corresponding to our rotating tank experiments. Thus this simulation demonstrates the possibility of producing a transitory square vortex in the rotating-tank under conditions similar to those in which the triangle was produced. The dimensional velocity and length scales and box size are as in figure 1. Thick (thin) lines represent positive (negative) contour levels. Panels are ordered from left to right, top to bottom, corresponding to times $t = 0, 80, 130$, and 140 s, and they have contour value increments of $\Delta\zeta = 0.8$, 0.4, 0.12, and 0.11 s^{-1}, respectively.

wavenumber 4 perturbation of amplitude $\mu = 0.125$. The square vortex formed after about 10 seconds. Unlike the triangle vortex which lasted indefinitely under the same conditions, this square vortex broke down after about two and a half rotations. The double satellite merger begins in the lower left panel. This led to an intermediate tripole state (lower right panel) which then broke down through the familiar double dipole instability. We also performed simulations in which the square vortex shown in figure 5 was perturbed by strengthening one satellite while correspondingly weakening another to preserve the total circulation. In those cases, only two satellites merged at first, leading to a temporary triangle vortex. Then another merger took place leading to the tripole state, and then finally the double-dipole instability took over. From these results, we conclude that it should be possible to observe a square vortex emerge from a nearly circularly symmetric vortex in rotating-tank experiments if the initial perturbation is made sufficiently close to a pure mode-4 perturbation. However, it is also clear that it would only appear as a transitory state.

We have also been able to create a pentagon vortex in a numerical simulation by a wavenumber-5 perturbation on an $\alpha = 8$ profile. Although strong satellites do form rapidly, the structure breaks down after executing only about half a rotation. The breakdown began with the nearly simultaneous merger of two pairs of satellites which produced a roughly triangular system. Another merger followed, producing a tripole state. The tripole finally broke up into a dipole and monopole.

Point – vortex models

Finally, we turn to the stability of the higher-order geometrical vortices, the square, the pentagon, etc., from the point of view of point-vortex models. Specifically, we consider here only the zero-circulation, steadily-rotating configurations, consisting of $n_s = n - 1$ equal strength point vortices symmetrically placed on a circle centred on a point vortex of opposite sign. It can be shown that the case $n = 3$, a model for the tripole, is nonlinearly stable to displacements (Kloosterziel 1990), and in Eckhardt (1988) it is shown that the case $n = 4$, the model of the triangular vortex, is also nonlinearly stable. Morikawa & Swenson (1971) performed a linear stability analysis on these models for all n. The perturbations they considered were small displacements in the initial positions. Consistent with the later nonlinear stability results, they found that the cases $n = 3$ and $n = 4$ are linearly stable, but more importantly, they proved that for all cases $n \geqslant 5$ the configurations are linearly unstable. For the cases $n = 5$ and $n = 6$, the models of the pentapole and hexapole, we have performed simulations that show that a 1% or less perturbation in the radial position of the satellites away from symmetry will result in the close approach of two of the satellites within one rotation period. This is the same form of instability that led to the close approach and merger of satellites in our simulations of the continuous pentapole and hexapole vortices. This should be contrasted with the case of the point-vortex model of the triangle, where perturbations of even 20% in the positions of the satellites can still be stable (Carnevale & Kloosterziel, 1994). In view of the results of Morikawa & Swenson (1971), we anticipate that all higher-order coherent continuous vortices are also unstable.

Conclusion

We have considered a hierarchy of isolated compound vortices in which the Lamb dipole and the tripole are the first two elements. The stability of these two structures is well known from experiments and simulations. Here we have reviewed evidence that the next element in this hierarchy, the quadrupole, is also stable, but with a much smaller instability threshold than the two lower-order structures. It seems that these three elements, dipole, tripole and quadrupole, are the only stable ones in the whole hierarchy. All of the higher-order compound vortices are expected to show the close approach and merger of two of the satellites, and subsequent breakup of the whole structure.

All of our simulations were performed with continuous vorticity profiles on a doubly periodic domain using a spectral code. Morel & Carton (1994) have performed a similar study based on contour dynamics, that is, simulations involving regions of piecewise constant vorticity. They also have found that the quadrupole is stable while higher order n-poles are not, thus adding to the weight of evidence for our conclusion.

Acknowledgements

This research has been supported in part by National Science Foundation grant OCE 91-21998 and Office of Naval Research grant N00014-93-1-0459. The numerical simulations were performed at the San Diego Super Computer Center. The laboratory experiments were performed in the Applied Mechanics and Engineering Sciences department at the University of California, San Diego.

References

Carnevale, G. F., M. Briscolini, R. Purini, & G.K. Vallis, 1988a - Numerical experiments on modon stability to topographic perturbations. *Phys. Fluids* **31**, 2562–2566.

Carnevale, G. F., Vallis, G.K., Purini, R., & Briscolini, M. 1988b Propagation of barotropic modons over topography. *Geophys. Astrophys. Fluid Dyn.* **41**, 45-101.

Carnevale, G.F., G.K. Vallis, R. Purini, & M. Briscolini, 1988c - The role of initial conditions in flow stability with applications to modons. *Phys. Fluids* **31**, 2567–2572.
Carnevale, G.F., J.C. McWilliams, Y. Pomeau, J.B. Weiss, & W.R. Young, 1991 - Evolution of vortex statistics in two-dimensional turbulence. *Phys. Rev. Letters* **64**, 2735–2737.
Carnevale, G.F., & R.C. Kloosterziel, 1994 - Emergence and evolution of triangular vortices. *J. Fluid Mech.* **259**, 305–331.
Carton, X.J., & J.C. McWilliams, 1989 - Barotropic and baroclinic instabilities of axisymmetric vortices in a quasi-geostrophic model. In: *Mesoscale/ Synoptic Coherent Structures in Geophysical Turbulence* (eds. J.C.J. Nihoul & B.M. Jamart), pp. 225–244, Elsevier.
Carton, X.J., G.R. Flierl, & L.M. Polvani, 1989 - The generation of tripoles from unstable axisymmetric isolated vortex structures. *Europhys. Lett.* **9**, 339–344.
Eckhardt, B., 1988 - Integrable four vortex motion. *Phys. Fluids* **31**, 2796–2801.
Federov, K.N., & A.I. Ginsburg, 1989 - Mushroom-like currents (vortex dipoles): one of the most widespread forms of non-stationary coherent motions in the ocean. In: *Mesoscale/ Synoptic Coherent Structures in Geophysical Turbulence* (eds. J.C.J. Nihoul & B.M. Jamart), pp. 1–14, Elsevier.
van Heijst, G.J.F., & R.C. Kloosterziel, 1989 - Tripolar vortices in a rotating fluid. *Nature* **338**, 569–561.
van Heijst, G.J.F., R.C. Kloosterziel, & C.W.M. Williams, 1991 - Laboratory experiments on the tripolar vortex in a rotating fluid. *J. Fluid Mech.* **225**, 301–332.
Kloosterziel, R.C., 1990 - *Barotropic Vortices in a Rotating Fluid.* PhD thesis, University of Utrecht, The Netherlands (209 pp.)
Kloosterziel, R.C., & G.J.F. van Heijst, 1991 - An experimental study of unstable barotropic vortices in a rotating fluid. *J. Fluid Mech.* **223**, 1–24.
Lamb, H., 1932 - *Hydrodynamics.* Cambridge University Press, 738 pp.
Legras, B., P. Santangelo, & R. Benzi, 1988 - High-resolution numerical experiments for forced two-dimensional turbulence. *Europhys. Lett.* **5**, 37–42.
McWilliams, J.C., 1980 - An application of equivalent modons to atmospheric blocking. *Dyn. Atmos. Oceans* **5**, 43–66.
McWilliams, J.C., G.R. Flierl, V.D. Larichev & G.M. Reznik, 1981 - Numerical studies of barotropic modons. *Dyn. Atmos. Oceans* **5**, 219–238.
Melander, M.V., N.J. Zabusky, & J.C. McWilliams, 1988 - Symmetric vortex merger in two-dimensions: causes and conditions. *J. Fluid Mech.* **195**, 303–340.
Morel, Y.G., & X.J. Carton, 1994 - Multipolar vortices in two-dimensional incompressible flows. *J. Fluid Mech.* **267**, 23–51.
Morikawa, G.K., & E.V. Swenson, 1971 - Interacting motion of rectilinear geostrophic vortices. *Phys. Fluids* **14**, 1058–1073.
Nycander, J., 1992 - Refutation of stability proofs for dipole vortices. *Phys. Fluids A* **4**, 467–476.
Orlandi, P., & G.J.F. van Heijst, 1992 - Numerical simulation of tripolar vortices in 2D flow. *Fluid Dyn. Res.* **9**, 170–206.

Pingree, R.D., & B. LeCann, 1992 - Three anticyclonic Slope Water Oceanic eDDIES (SWODDIES) in the Southern Bay of Biscay in 1990. *Deep Sea Res.* **39**, 1147–1175.
Polvani, L.M., & X.J. Carton, 1990 - The tripole: a new coherent vortex structure of incompressible two-dimensional flows. *Geophys. Astrophys. Fluid Dyn.* **51**, 87–102.
Sadourny, S., 1985 - Quasi-geostrophic turbulence: an introduction. In: *Turbulence and Predictability in Geophysical Fluid Dynamics and Climate Dynamics* (M. Ghil ed.), North Holland, Amsterdam, pp. 133–158.
Stern, M.E., 1975 - Minimal properties of planetary eddies. *J. Mar. Res.* **33**, 1–13.

+ Scripps Institution of Oceanography
La Jolla, CA 92093, USA

° University of Hawaii
School of Ocean and Earth Science and Technology
Department of Oceanography
Honolulu, Hawaii 96822, USA